Catalysis Today 148 (2009) 232–242

Contents lists available at ScienceDirect

Catalysis Today

journal homepage: www.elsevier.com/locate/cattod

Using tapered element oscillating microbalance for in situ monitoring of carbon deposition on nickel catalyst during CO_2 reforming of methane

Wei Pan, Chunshan Song *

Clean Fuels and Catalysis Program, EMS Energy Institute, and Department of Energy & Mineral Engineering, The Pennsylvania State University, 209 Academic Projects Building, University Park, PA 16802, USA

ARTICLE INFO

Article history:
Available online 5 November 2009

Keywords:
CO_2 reforming
Ni/Al_2O_3
Catalyst
Carbon formation
Tapered element oscillation microbalance (TEOM)

ABSTRACT

The present work aims at clarifying the carbon formation behavior through an in situ monitoring of carbon deposition on Ni/Al_2O_3 catalyst during CO_2 reforming of methane using the tapered element oscillating microbalance (TEOM). The carbon deposits were also characterized by transmission electron micrograph (TEM) and temperature-programmed oxidation with IR detector (TPO-IR). TEOM results and a kinetic study on carbon formation established that both CO in the products and CH_4 in the reactants can be the source of carbon formation during the CO_2 reforming reaction. In an equimolar CO_2–CH_4 reforming condition, CO in the product stream is likely the major source of carbon formation. TEM coupled with TPO-IR and TEOM revealed that carbon formed in CO_2 reforming from a feed without containing CO shows more filamentous carbon, which is more difficult to be oxidized, while carbon formed from a feed containing CO mostly encapsulates metal particles in the catalyst and is relatively easy to be oxidized. Replacing some of CO_2 with H_2O greatly inhibits carbon formation encountered in CO_2 reforming. Kinetic studies with TEOM showed that H_2 addition to the feed gas can enhance carbon formation from CH_4, probably by hydrogenating surface carbon species and clean the surface metal sites active for methane decomposition; addition of CO to the feed gas $CH_4 + CO_2$ can further enhance carbon formation more than that with H_2 addition alone; whereas H_2O addition can reduce carbon formation from both CO and CH_4, most likely by gasifying carbon species.

1. Introduction

Carbon dioxide (CO_2) can be reduced and utilized as carbon monoxide (CO), methane (CH_4), and methanol (CH_3OH) as well as other chemicals and materials [1–4]. The reaction of CO_2 reforming of methane converts CO_2 by methane into CO and H_2. This reaction was initially proposed for using CO_2 to produce industrially useful CO and H_2 [5] which is also viewed as one way to reduce emissions of CO_2, a greenhouse gas. However, the application of CO_2 reforming of methane is not nearly as successful as steam reforming process because catalysts in CO_2 reforming have limited lifetime due to severe carbon deposition problems. Carbon deposition can lead to catalyst disintegration and deactivation. In addition, CO_2 reforming is a more endothermic reaction compared to steam reforming, thus requiring a significant energy input. This reaction would need a supply of CO_2 which is not readily available and require separation and recovery of CO_2 on-site in manufacturing plants. On the other hand, CO_2 reforming can also be used for converting and utilizing CO_2-rich natural gas [6] as some natural gas resources contain up to 50 vol% CO_2 which are not yet utilized commercially due to the high CO_2 concentrations. Furthermore, the recently developed concept for tri-reforming of methane including CO_2 reforming can be used for converting CO_2-rich natural gas or CO_2-rich bio-gas, or for converting natural gas along with flue gas of natural gas-fired or coal-fired electric power plants [6,7]. Tri-reforming process concept was recently proposed and developed at the Pennsylvania State University [6,7], and established by independent studies on tri-reforming catalysts and process worldwide [8–11]. Tri-reforming is a synergetic combination of CO_2 reforming, steam reforming and partial oxidation of methane [4,6]. CO_2 reforming may also be used for conversion and utilization of bio-gas such as anaerobic digester gas and landfill gas which contain up to 40–50% CO_2 in addition to methane. General aspects of catalytic CO_2 reforming have been reviewed by Bradford and Vannice in 1999 [12] and more recently by Hu and Ruckenstein in 2004 [13].

The present study deals with CO_2 reforming of methane with a focus on the problem of carbon formation in this reaction process. In the system of CO_2 reforming of methane, there exist the same five gases (e.g., CO_2, CH_4, H_2O, CO, and H_2) as those in the system of steam reforming. The tri-reforming and other combined reforming including CO_2 reforming, steam reforming and partial oxidation

* Corresponding author. Tel.: +1 814 863 4466; fax: +1 814 865 3248.
E-mail address: csong@psu.edu (C. Song).

0920-5861/$ – see front matter © 2009 Published by Elsevier B.V.
doi:10.1016/j.cattod.2009.09.002

may also involve the oxidation reactions by O_2. The related reactions are shown in Eqs. (1)–(8). A major difference between the CO_2 reforming and steam reforming systems is the relative concentration of each component in these two reaction processes at different conversion levels. Assuming both steam reforming and CO_2 reforming start from the reactant gas mixtures of $H_2O/CH_4 = 1$ and $CO_2/CH_4 = 1$ with CH_4 conversion of 80% and assuming water gas shift reaction and other side reactions are negligible, then the gas mixture after steam reforming will contain about 22% CO, 67% H_2, 5.5% CH_4 and 5.5% H_2O, while the gas mixture after CO_2 reforming will contain 44% CO, 44% H_2, 5.5% CO_2 and 5.5% CH_4 at about 720 °C and 1 atm.

One of the major problems in CO_2 reforming is the carbon deposit formation [2,3]. In CO_2 reforming reaction, the possible routes to form carbon includes methane decomposition (Eq. (6)); and/or CO disproportionation (Eq. (7)). The clarification of this issue is necessary because it will help to understand the mechanism of carbon formation in this reforming reaction and provide the insight that will be beneficial for the design of reactor as well as the design of stable and carbon-resistant catalysts.

CO_2 reforming of methane

$$CO_2 + CH_4 = 2CO + 2H_2 \quad \Delta H^\circ = +247.3\,\text{kJ/mol} \tag{1}$$

Steam reforming of methane

$$H_2O + CH_4 = CO + 3H_2 \quad \Delta H^\circ = +206.3\,\text{kJ/mol} \tag{2}$$

Partial oxidation of methane

$$(1/2)O_2 + CH_4 = CO + 2H_2 \quad \Delta H^\circ = -35.6\,\text{kJ/mol} \tag{3}$$

Complete oxidation of methane

$$2O_2 + CH_4 = CO_2 + 2H_2O \quad \Delta H^\circ = -880\,\text{kJ/mol} \tag{4}$$

Water gas shift reaction

$$CO + H_2O = CO_2 + H_2 \quad \Delta H^\circ = -41\,\text{kJ/mol} \tag{5}$$

Methane decomposition

$$CH_4 = C + 2H_2 \quad \Delta H^\circ = +75\,\text{kJ/mol} \tag{6}$$

CO Disproportionation

$$2CO = C + CO_2 \quad \Delta H^\circ = -172\,\text{kJ/mol} \tag{7}$$

Deoxygenation of CO

$$CO + H_2 = C + H_2O \quad \Delta H^\circ = -131\,\text{kJ/mol} \tag{8}$$

Wang and Lu [14] studied the dependence of carbon formation rate (R_c) on partial pressure of CH_4 (P_{CH_4}) and CO_2 (P_{CO_2}) in CO_2 reforming of methane, the reaction order of carbon formation rate with respect to CO_2 partial pressure (shown in Eq. (9)) is negative, indicating that CO_2 in the feed inhibits carbon deposition. Hence, Wang and Lu [14] concluded that methane decomposition is the main route for carbon deposition in CO_2 reforming over Ni/γ-Al_2O_3 catalysts.

$$R_c = K_c P_{CH_4}^{1.18} P_{CO_2}^{-0.68} \tag{9}$$

By analyzing their measurement conditions, we estimate that their carbon formation rates were measured under differential reaction conditions (space velocity is about 1,440,000 h^{-1} and contact time (W/F) is around 0.015 g h mol^{-1}) although the methane conversion is not mentioned in the paper. It is expected that very little CO is produced in their studied system. Therefore, the effect of CO on carbon formation has not been fully taken into consideration in their study.

In addition, if methane decomposition is the main route of carbon formation in CO_2 reforming, it is difficult to explain the experimental phenomenon observed by Fujimoto and co-workers [15] that carbon formation increases with the increase of reaction pressures (1–20 atm). Thermodynamically, higher reaction pressures do not favor methane decomposition itself.

On the other hand, several researchers [16–19] suggest that CO disproportionation is responsible for carbon formation in CO_2 reforming. CO disproportionation is an exothermic reaction. The equilibrium carbon formation will increase with increasing pressure and decrease with increasing temperature. This explains well the pressure effect on carbon formation observed by Fujimoto and co-workers [20]. It also agrees well with the temperature effect observed by Zhang and Verykios [18] and Richardson and Paripatyadar [17]. They observed that the amount of carbon on Ni/γ-Al_2O_3 and Ru or Rh/Al_2O_3 after 2 h or 8 h reaction decreased with the increase of reaction temperatures even starting from 500 °C or 610 °C. Fujimoto and co-workers [20] reported that carbon formation after 4 h reaction over NiO–MgO solid-solution catalysts decreased when temperature was increased from 800 °C to 900 °C. However, there is barely a direct experimental evidence to prove that CO is responsible for carbon formation in CO_2 reforming. Swaan et al. [21] used isotope labeling and TPO (ex situ approach) and reported that carbon formed during CO_2 reforming of methane may be from both CH_4 and CO_2.

Through experimental research in our laboratory, we believe that the experimental methods and conditions employed to study carbon formation are critical to correctly understand carbon formation behavior. For example, the method to measure carbon formation, in situ or ex situ, makes a difference. Ex situ techniques may not provide accurate information. For another example, in a fixed-bed flow reactor, when CO_2 reforming reaction reaches close to equilibrium, the gas phase compositions along the catalyst bed are different. Near the outlet of the catalyst bed, the gas phase contains not only unconverted CH_4 and CO_2, but also products such as CO and H_2. The appearance of CO [22] and H_2 [23] together with CH_4 and CO_2 in the gas phase might affect the carbon formation behavior and carbon morphology. It is possible that the experiments done in some previous studies [14] did not reflect the carbon formation behavior in real CO_2 reforming process because the experiments were conducted at very low CH_4 conversions and there was almost no CO present in the gas phase. To study carbon formation in CO_2 reforming, gas phase composition should be close to those in a reformer containing both CH_4 and CO.

In the present work, we have employed a very useful in situ technique, Tapered Element Oscillation Microbalance (TEOM), to monitor the dynamic process of carbon formation in real CO_2 reforming conditions. TEOM will enable us to measure in situ carbon formation under continuous-flow reaction conditions and to perform the kinetic study of carbon formation at different CH_4 and CO partial pressures.

2. Experimental

2.1. Nickel catalyst

The nickel catalyst used is a commercial NiO/α-Al_2O_3 catalyst from ICI (Synetix 23-4, R15513). Johnson Matthey acquired Synetix catalyst business from ICI in 2003 and Synetix reforming catalysts are now available as Katalco catalysts. Table 1 shows the physicochemical properties of the ICI Synetix 23-4 nickel catalyst. The nickel particle size was determined by XRD of the reduced catalyst.

2.2. TEOM measurement

The TEOM (Rupprecht & Patashnick, Co., Inc.) is a useful instrument capable of monitoring carbon formation in situ at high temperatures (up to 700 °C) and high pressures (up to 68 atm). It was

Table 1
Physico-chemical properties of the nickel catalyst.

Catalyst	NiO loading (wt.%)	Specific surface area by single point BET method (m^2/g)	Specific surface area by multi-point BET method (m^2/g)	Average Ni particle size by XRD (nm)
Synetix 23-4	23	3.4	4.4	44.1

modified and integrated into the catalyst performance test system as shown in Fig. 1. The exit gas from the TEOM can be analyzed by an on-line gas chromatograph (SRI instruments) as well.

The TEOM measures the weight change of a sample in situ by comparing the vibrating frequency of the tapered glass sample cell during the measurement. At the beginning of an analysis, the sample cell vibrates in a set frequency depending on its mass. When there is mass change of the sample, the vibration frequency of the sample cell consequently changes. The frequency change of the sample cell is detected by an optical device and converted into the mass change based on the following equation (Eq. (10)).

$$\Delta_m = \frac{k}{f_1^2} - \frac{k}{f_0^2} \tag{10}$$

where k = constant for a specific TEOM apparatus, f_0 and f_1 = the frequencies of the glass sample cell at the measurement time of t_0 and t_1, respectively.

A catalyst sample was loaded into the tip of the tapered glass cell (reactor) and supported and fixed by quartz wool and a metal cap coated with gold. The glass cell was protected by a stainless steel tube. The temperature of the TEOM was controlled by the temperature control unit and software. The pressures in the system and the flows of input gases were controlled by a back pressure regulator (TESCOM) and mass flow controllers (Brooks), respectively. Distilled water was pumped into the system by the ISCO syringe pump (Model 500D). A purge gas (Ar, 100 ml/min) was used to sweep outside the glass cell in order to carry the effluent from the reactor out of the system and, in the meantime, to prevent effluent from flowing into the optical devices.

One of the major advantages of the TEOM compared with conventional gravimetric microbalance systems is that the configuration of the TEOM enables all reactants to pass through the catalyst bed inside the glass sample cell just like in a fixed-bed reactor, avoiding the problems of gas by-pass and buoyancy which are often encountered in a conventional TGA (thermo-gravimetric analysis) measurement. Demicheli et al. [24] noticed that a high flow rate of feed could affect the weight variation measurements using a TGA apparatus. Therefore, the feed gas flow rates were limited to a very low range. Kroll et al. [25] observed a large discrepancy of carbon deposition measured by the TGA and by TPH/TPO over catalyst samples after different time-on-stream in a reactor. They attributed this discrepancy to the higher temperature gradients throughout the catalyst bed in the TGA due to the gas by-pass. Their microbalance was equipped with a perforated basket instead of a plug-flow fixed-bed reactor.

The in situ measurement of carbon deposition by the TEOM provides more accurate information on carbon formation behavior than ex situ approaches such as TPH and TPO, especially when the carbon formation rate changes with the time-on-stream.

The TEOM experiments in this paper were carried out at 650 °C and 1 atm. Prior to each measurement, 12–50 mg ICI Ni/Al_2O_3 catalyst (35–60 mesh) was loaded into the glass tube and reduced by 40% H_2 in Ar (5 ml/min H_2 + 7.5 ml/min Ar) at 100 °C for 10 min, 450 °C for 75 min, and 650 °C for 30 min. The heating rate from room temperature to 100 °C, from 100 °C to 450 °C, and from 450 °C to 650 °C was 12 °C/min. After the reduction, the catalyst was purged with Ar (7.5 ml/min) for 10 min, followed by the preparation of reactant gases in another line. After another 5 min, the prepared gases were switched into the TEOM and the monitoring of mass changes started. When the mass change was found to be over 15 wt.% of the sample, the experiment was stopped to protect the glass cell from damage.

In the case where H_2O was used for the experiment, H_2O was pumped into the TEOM through a separate line which is connected to the preheating zone of the TEOM. The gases and vaporized steam in the preheating zone were mixed and flowed into the TEOM.

2.3. Carbon analyzer

The amount of carbon deposited on the catalysts after TEOM experiments could be determined using a carbon analyzer (LECO RC-412) as well. 10–20 mg catalyst after reforming reactions was

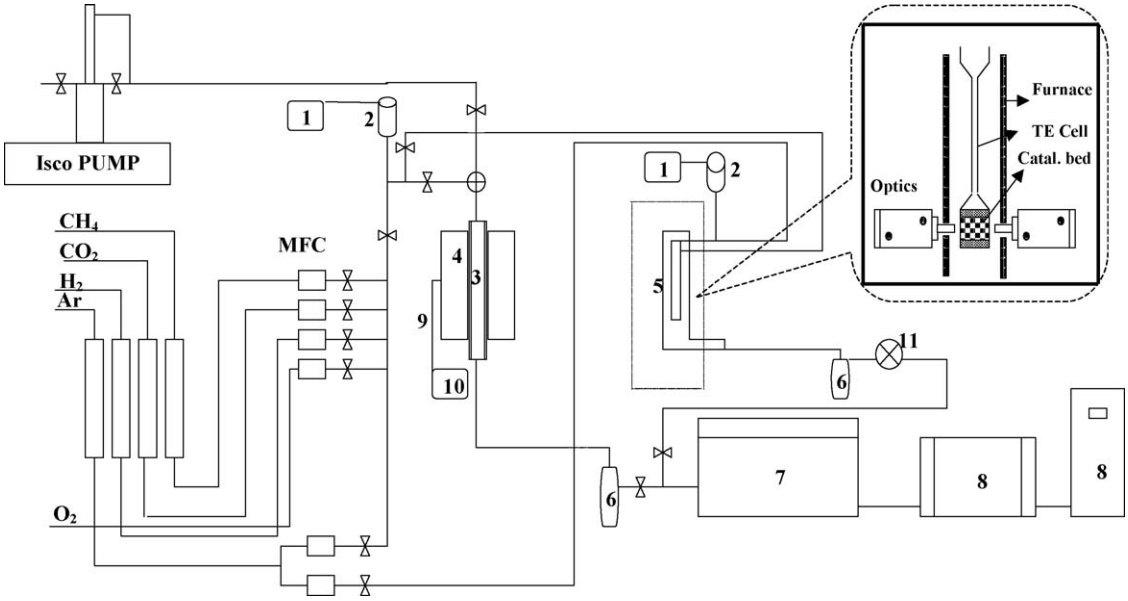

Fig. 1. Schematic diagram of integrated tri-reforming reactor/TEOM reactor. (1) Pressure indicator, (2) pressure transducer, (3) tri-reforming reactor, (4) furnace, (5) TEOM reactor, (6) condenser, (7) GC, (8) computer, (9) thermocouple, (10) temperature indicator, (11) backpressure regulator (MFC: mass flow controller).

loaded into the sample holder and put in the heating zone purged by O_2 (750 ml/min). After the start of analysis, the temperature of the heating zone was increased from 100 °C to 900 °C at a heating rate of 30 °C. When the heating zone temperature reached a certain high temperature which depends on the nature of carbon in the sample, carbon on the sample could be oxidized into CO_2. The produced CO_2 was detected by an IR detector and the amount of carbon on the sample could be calibrated by comparing with the standard sample (LECO calibration sample with 1.03% carbon content). The temperature at which carbon is oxidized could provide information on the reactivity of carbon on the sample towards oxidation.

2.4. TEM and SEM

The morphology of carbon on Ni/Al_2O_3 catalyst (ICI Syntix 23-4) after CO_2 reforming were further determined by TEM (point-to-point resolution of 1 nm) using an ultrasonically dispersed (in ethanol) catalyst sample deposited on a thin carbon film supported on a standard copper grid. The TEM (JEOL JEM 1200 EXII) is interfaced with a video camera and a high resolution Tietz F224 camera. The accelerating voltage during the scanning was 80 kV.

The morphology of Ni particles on Ni/Al_2O_3 catalyst (ICI catalyst) after reduction at 850 °C and the morphology of carbon formed on this catalyst surface after CO_2 reforming reaction were examined by SEM (HITACHI S-3500N). Two or three catalyst particles in the size of ca. 0.2–2 mm were adhered to the SEM sample holder by carbon tape. To avoid a charging problem during the scanning, all the SEM samples were treated with a conductive coating of gold. The treated sample was then loaded into the SEM detection chamber equipped with a secondary electron detector, a backscattered electron detector, and energy dispersive X-ray spectroscopy (EDS) with both PGT (Princeton Gamma-Tech) PRISM Si(Li) detector and IMIX-PC Analyzer system.

3. Results and discussion

3.1. Thermodynamic analysis of carbon formation from CH_4 or CO

Since both CH_4 and CO are possible sources for carbon formation during the CO_2 reforming reaction, the thermodynamic behavior of carbon formation from CH_4 decomposition and CO disproportionation was first studied using the commercial HSC Chemistry program.

CH_4 decomposition is an endothermic reaction. Carbon formation is favored at higher temperatures as shown in Fig. 2. On the contrary, CO disproportionation is an exothermic reaction. Equilibrium CO conversion and carbon formation decline with the increase of reaction temperature (Fig. 3).

In practice, CH_4 decomposition and CO disproportionation are often conducted over catalysts due to the kinetics of these reactions. It has been found that carbon formed in CH_4 decomposition and CO disproportionation over catalysts may not be in the form of graphite and has higher free energy compared with graphite [26,27]. The difference of the free energy between carbon on catalysts and graphite becomes smaller when carbon on catalysts is obtained at reaction temperatures higher than 600 °C.

To demonstrate the effect of thermodynamic properties of carbon on catalysts on the equilibrium of methane decomposition and CO disproportionation, free energy data of carbon on Ni catalysts reported in Dent's paper [26] is used for calculation. The results are compared with those calculated based on graphite (Figs. 2 and 3). The comparison reveals that the high free energy of carbon on Ni catalysts results in the lower conversions of CH_4 and CO, as well as lower carbon formation in both CH_4 decomposition and CO disproportionation reactions. For example, the biggest

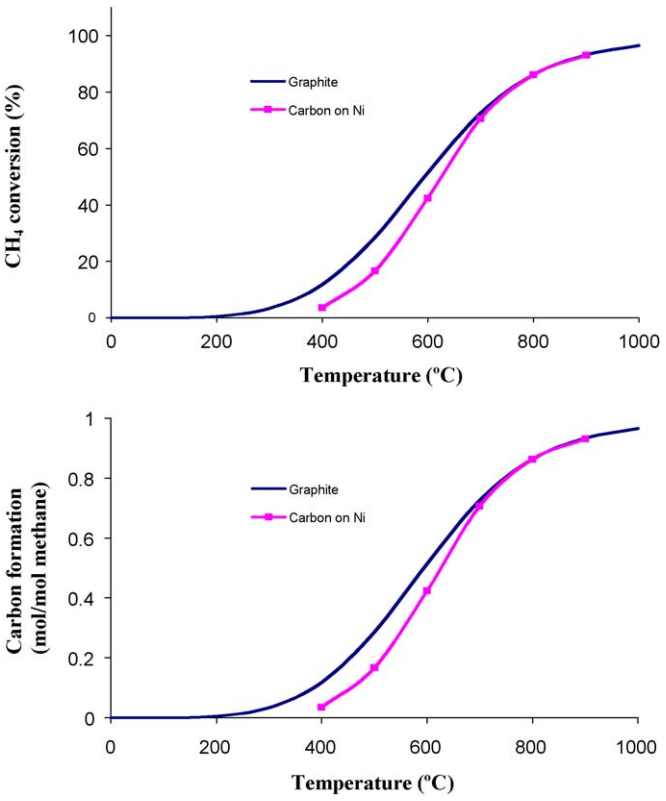

Fig. 2. Difference of CH_4 conversion and carbon formation in $CH_4 = C$ (graphite) + $2H_2$ and $CH_4 = C$ (carbon on nickel) + $2H_2$. The free energy of carbon on nickel catalysts is derived from Dent et al. (1945–1946) [26].

difference in CH_4 conversion and carbon formation is observed at 500 °C in the CH_4 decomposition reaction. At 500 °C, equilibrium CH_4 conversion and carbon formation from 1 mol of methane based on graphite are about 28.6% and 0.286 mol, respectively,

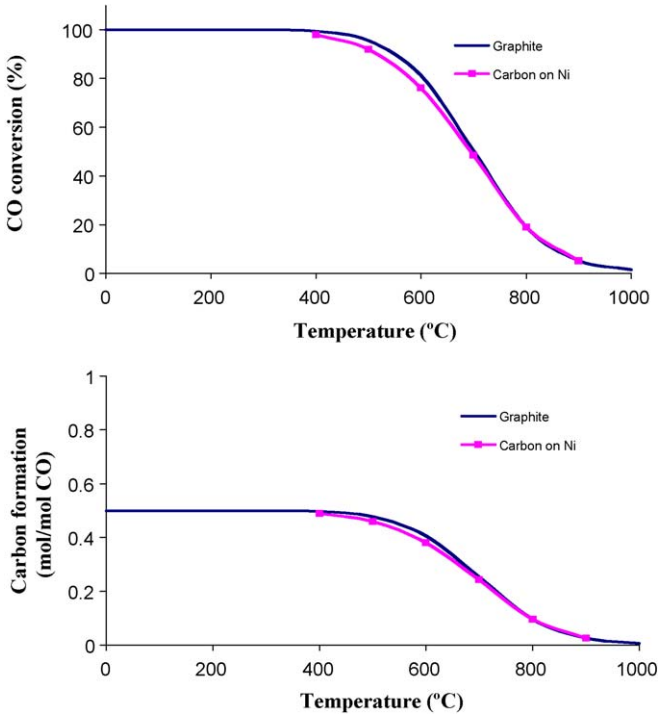

Fig. 3. Difference of CO conversion and carbon formation in $2CO = C$ (graphite) + CO_2 and $2CO = C$ (carbon on nickel) + CO_2. The free energy of carbon on nickel catalysts is derived from Dent et al. (1945–1946) [26].

while equilibrium CH_4 conversion and carbon formation based on carbon on Ni catalysts is only 16.7% and 0.167 mol, respectively. However, with the increase of temperature, these differences gradually disappear because the free energy of carbon on Ni catalysts becomes close to that of graphite.

Based on these observations, it was decided to use the thermodynamic properties of graphite for our thermodynamic analysis in CO_2 reforming because this reaction has applicable conversions only at temperatures above 700 °C. At temperatures above 700 °C, the difference of free energy between graphite and carbon on catalysts becomes small and the effect of this difference on thermodynamic analysis is negligible.

3.2. Thermodynamic analysis of carbon formation in CO_2 reforming of methane

Fig. 4 shows the equilibrium carbon formation in CO_2 reforming of methane. Instead of analyzing each individual carbon formation reaction, our thermodynamic analysis considers all the possible reactions during the real CO_2 reforming system. In a practical CO_2 reforming system, CO_2–CH_4 reforming reaction as well as side reactions such as water gas shift reaction and carbon formation reactions take place simultaneously. In order to obtain equilibrium compositions, the Gibbs energy minimization method was employed [28] and minimization was carried out using the commercial HSC Chemistry program.

In a CO_2 reforming reaction system, there exist at least six components, including CO_2, CH_4, CO, H_2, H_2O, and C. Based on the mass balance of three elements (C, H, and O), three equations can be established. In addition, according to the rule described by Denbigh [28], the number of independent reactions in a reaction system can be determined by writing down the formation equations of all compounds in the reaction system from their elemental atoms, followed by combining these equations in such a way as to eliminate any free atoms which are not actually present. As a result, in the CO_2 reforming system, there are three independent reactions which can be expressed as three equilibrium equations. Therefore, theoretically, the equilibrium composition in the CO_2 reforming system can also be obtained by solving the six equations.

It can be seen from Fig. 4 that the trend of carbon formation with the increase of temperature in CO_2 reforming is similar to that observed in Fig. 3. Higher carbon formation at low temperatures and lower carbon formation at higher temperatures suggest that CO disproportionation probably dictates equilibrium carbon formation in the CO_2 reforming reaction. This seems reasonable because CO is the dominant source to produce carbon at lower temperatures. The CO disproportionation reaction has large equilibrium constant towards carbon formation at low temperatures due to the highly exothermic property of this reaction. At higher temperatures, most of the CH_4 may react with CO_2 and form CO; as a result, little methane is left. Hence, CO still largely determines the equilibrium carbon formation at higher temperatures in a CO_2 reforming system.

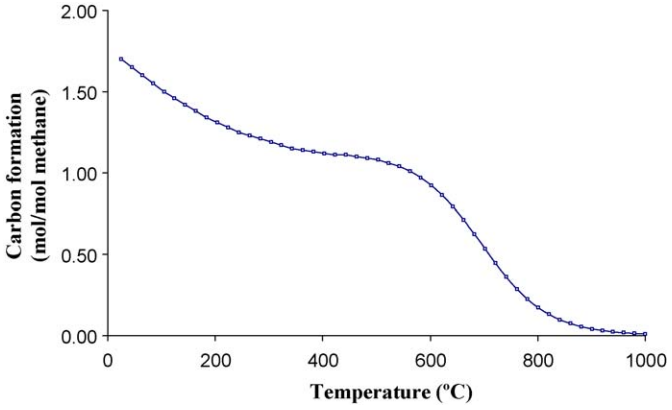

Fig. 4. Theoretical calculation of carbon formation in CO_2 reforming of methane.

3.3. TEOM measurement of carbon formation in CO_2 reforming of methane

Carbon formation in the CO_2 reforming of methane with CH_4/CO_2 (mol ratio) = 1 was measured by the TEOM at 650 °C and 1 atm over 25 mg ICI catalyst. To investigate the effect of CO in the product on carbon formation during CO_2 reforming, feed containing CO was also tested to simulate the gas composition at 25% and 50% methane conversions in CO_2 reforming. Fig. 5 shows the amount of carbon with the time-on-stream at the following three different gas compositions: CH_4:CO_2:CO:H_2 (mol ratio) = 1:1:0:0, 0.75:0.75:0.5:0.5, and 0.5:0.5:1:1. When the feed contains only CO_2 and CH_4 (CH_4:CO_2:CO:H_2 = 1:1:0:0), carbon was observed to form at a constant rate of 5.6 μg/s/g cat. (microgram carbon per second per gram catalyst). When feed contains CH_4:CO_2:CO:H_2 = 0.75:0.75:0.5:0.5, the carbon formation rate increased dramatically to 155.3 μg/s/g cat., almost 30 times higher than the carbon formation rate at CH_4:CO_2:CO:H_2 = 1:1:0:0. With more CO present in the feed (CH_4:CO_2:CO:H_2 = 0.5:0.5:1:1), the carbon formation rate increased even further, up to 420.1 μg/s/g cat. These results clearly indicate that CO in the product stream of CO_2 reforming contributes greatly to carbon formation in CO_2 reforming. The possible reasons for the increase of carbon formation when CO is present in CO_2 reforming include: (1) Carbon species from CH_4 dissociation may readily react with CO_2 or surface oxygen derived from CO_2 into CO while carbon species from CO are probably less active [22]. (2) One mole of CH_4 and one mole of CO_2 can produce stoichiometrically two moles of CO. The amount of CO in the product is almost twice the amount of CH_4 converted. (3) H_2 is less active than CO_2 to remove carbon [29]. At high CH_4 conversions, less CO_2 is left.

3.4. TPO analysis of carbon formation in CO_2 reforming

From the TEOM measurements (Fig. 5), it is possible to estimate the weight percentage of carbon formed on ICI catalyst after a certain time-on-stream. When there is no CO in feed (CH_4:CO_2:CO:H_2 (mol ratio) = 1:1:0:0), 4.51 wt.% of carbon was formed on the catalyst after about 1.5 h. If the feed contains CO, much less

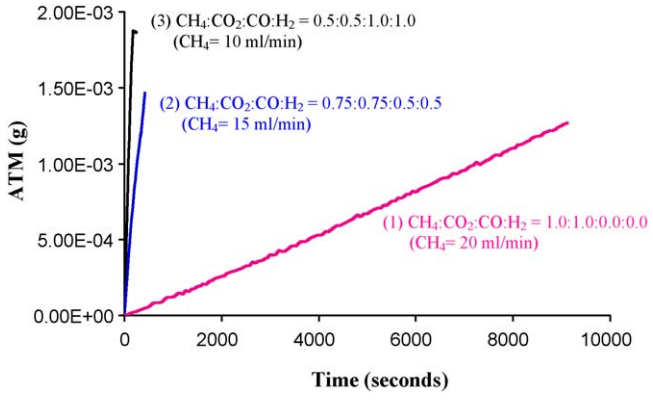

Fig. 5. Carbon formation at 1 atm and 650 °C over 25 mg Ni/Al_2O_3 (ICI Syntix 23-4) catalyst at different feed gas compositions simulating (1) initial CO_2 reforming CO_2:CH_4 (mol ratio) = 1:1, 1.5 h (2) 25% CO_2 reforming conversion, 6 min (3) 50% CO_2 reforming conversion, 3 min.

time is required to obtain a similar amount of carbon. 5.81 wt.% of carbon was deposited on catalyst in about 6 min when feed contains CH_4:CO_2:CO:H_2 (mol ratio) = 0.75:0.75:0.5:0.5, while 7.35 wt.% of carbon was formed in less than 3 min (Fig. 5) with the feed containing CH_4:CO_2:CO:H_2 (mol ratio) = 0.5:0.5:1:1. After about 1.5 h, 6 min, and 3 min of reaction during the TEOM experiments at CH_4:CO_2:CO:H_2 = 1:1:0:0, 0.75:0.75:0.5:0.5, and 0.5:0.5:1:1, respectively, reactants were switched to inert gas (such as Ar) to purge the catalyst bed and stop further carbon formation. The catalyst samples were then removed from the TEOM sample cell after they were cooled to room temperature. These samples were further analyzed by a carbon analyzer, TPO-IR, in order to determine the nature of carbon formed on these catalysts. Since the TPO-IR is capable of determining the amount of carbon formation on catalysts as well, the amount of carbon determined by the TPO-IR was compared with that from the TEOM to confirm the capability of the TEOM for in situ carbon formation measurement.

Fig. 6 shows the TPO-IR profiles of three samples after TEOM experiments at CH_4:CO_2:CO:H_2 = 1:1:0:0 for 1.5 h, CH_4:CO_2:CO:H_2 = 0.75:0.75:0.5:0.5 for 6 min, and CH_4:CO_2:CO:H_2 = 0.5:0.5:1:1 for 3 min. It was noticed that there is only one distinguishable oxidation peak on all three samples. The sample after the TEOM test at CH_4:CO_2:CO:H_2 = 1:1:0:0 shows the highest oxidation peak temperature at 595 °C while the oxidation peaks occur at 552 °C and 547 °C, respectively, over the other two samples after the TEOM experiment at CH_4:CO_2:CO:H_2 = 0.75:0.75:0.5:0.5 and 0.5:0.5:1:1. Chang and co-workers [30] observed only one oxidation peak at ca. 600 °C in the TPO profiles of spent supported Ni catalysts used in CO_2–CH_4 reaction at 700 °C for several hours. However, Goula and co-workers [31] showed two oxidation peaks at 610 °C and 700 °C, respectively, in the TPO profiles over Ni/CaO/Al_2O_3 catalyst after CO_2 reforming at 750 °C for 5 min. Olsbye et al. [32] reported only one TPO peak at ca. 700 °C over La_2O_3 promoted Ni/Al_2O_3 catalysts, but two TPO peaks at 650–700 °C and >800 °C, respectively, over Ni/Al_2O_3 after 114 h reaction at 700–900 °C in a CO_2–CH_4 reforming reaction. Shamsi and Johnson [33] observed two peaks in TPO profiles over Pt/CeZrOx catalyst after CO_2–CH_4 reforming at 800 °C. Besides the high temperature TPO peak at ca. 700 °C, a TPO peak at a temperature as low as 380 °C was even observed.

The TPO results from Wang and Lu [34] indicated that the oxidation peak position in TPO profiles depends on the supports of the catalysts as well. On Ni/α-Al_2O_3, the carbon oxidation peak was at 620 °C, while on Ni/MgO it was at about 650 °C. Carbon formed over Ni/γ-Al_2O_3 and Ni/SiO_2 catalysts was more difficult to oxidize, with the peaks occurring around 700 °C.

The TPO peak temperature of 595 °C on the ICI catalyst after reaction at CH_4:CO_2:CO:H_2 = 1:1:0:0 for 1.5 h is generally similar

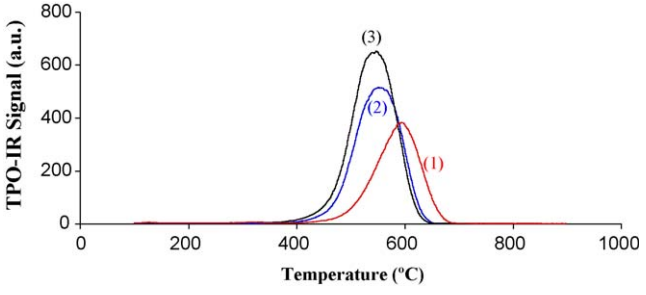

Fig. 6. TPO-IR profiles of carbon formed at 1 atm and 650 °C over 25 mg Ni/Al_2O_3 (ICI Syntix 23-4) catalyst at different feed gas compositions simulating (1) initial CO_2 reforming (CH4:CO_2:CO:H_2 = 1:1:0:0), 1.5 h (2) 25% CO_2 reforming conversion (CH_4:CO_2:CO:H_2 = 0.75:0.75:0.5:0.5), 6 min. (3) 50% CO_2 reforming conversion (CH_4:CO_2:CO:H_2 = 0.5:0.5:1:1), 3 min.

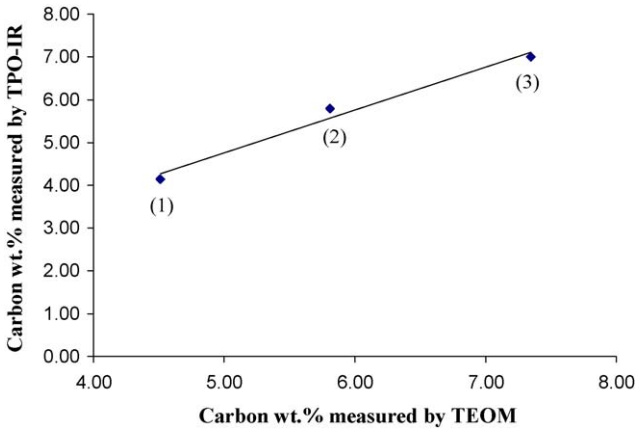

Fig. 7. Comparison of the weight percentage of carbon formation measured by TEOM and TPO-IR (Carbon Analyzer) after reaction over 25 mg Ni/Al_2O_3 (ICI Syntix 23-4) catalysts at 1 atm and 650 °C at different feed gas compositions simulating (1) initial CO_2 reforming (CH_4:CO_2:CO:H_2 = 1:1:0:0), 1.5 h. (2) 25% CO_2 reforming conversion (CH_4:CO_2:CO:H_2 = 0.75:0.75:0.5:0.5), 6 min. (3) 50% CO_2 reforming conversion (CH_4:CO_2:CO:H_2 = 0.5:0.5:1:1), 3 min.

to the TPO peak temperatures reported in the literature [34]. However, the ICI catalysts after the reaction at CH_4:CO_2:CO:H_2 = 0.75:0.75:0.5:0.5 and 0.5:0.5:1:1 showed relatively lower TPO peak temperatures close to 550 °C, indicating that carbon formed on the catalyst after reaction at CH_4:CO_2:CO:H_2 = 1:1:0:0 have a more ordered structure. This is supported by the TEM results which will be discussed in the next section.

Fig. 7 compares the weight percentages of carbon estimated by the TEOM and by the TPO-IR on the samples after reaction with the feed gas of CH_4:CO_2:CO:H_2 = 1:1:0:0, 0.75:0.75:0.5:0.5, and 0.5:0.5:1:1. The good linear correlation between these two demonstrates that the TEOM and TPO-IR results are consistent and the TEOM is a useful technique capable for studying dynamic process of carbon formation on catalysts.

3.5. TEM and SEM analysis on carbon formed on catalysts after CO_2 reforming of methane

The TPO-IR results in Fig. 6 indicated that carbon formed with different gas compositions has different reactivity towards oxidation. To further elucidate these differences, SEM and TEM were employed to characterize the carbon formed over the spent ICI catalysts after reforming reaction at 1 atm and 650 °C at CH_4:CO_2:CO:H_2 = 1:1:0:0 for 1.5 h, CH_4:CO_2:CO:H_2 = 0.75:0.75:0.5:0.5 for 6 min, and CH_4:CO_2:CO:H_2 = 0.5:0.5:1:1 for 3 min.

Fig. 8 shows the SEM images of the spent Ni/Al_2O_3 (ICI) catalysts after CO_2 reforming with different feed compositions. Although there was about 4.0–7.0 wt.% carbon formed on the ICI catalyst as confirmed by the TEOM and TPO-IR measurements, no obvious difference was observed in these SEM images. However, in the TEM images below, the difference among these samples is apparent.

Fig. 9 shows the TEM images of the morphology of some carbon formed on the Ni/Al_2O_3 (ICI) catalyst after reaction at 1 atm and 650 °C at CH_4:CO_2:CO:H_2 = 1:1:0:0 for 1.5 h. The amount of accumulated carbon is about 4.1–4.5 wt.%. Various kinds of carbon morphology were observed, indicating that carbon formation is quite a heterogeneous process on catalyst even though the average rate of carbon formation is almost constant, as shown in Fig. 5. Besides encapsulating carbon, Fig. 9(A) shows a cylinder-shaped carbon with layer structure and a diameter of ca. 60 nm. Fig. 9(B) illustrates the existence of encapsulating carbon deposits which cover the catalyst particles. Fig. 9(C)–(E) shows different shapes and length of filamentous carbon. It is noticed that all the filamentous

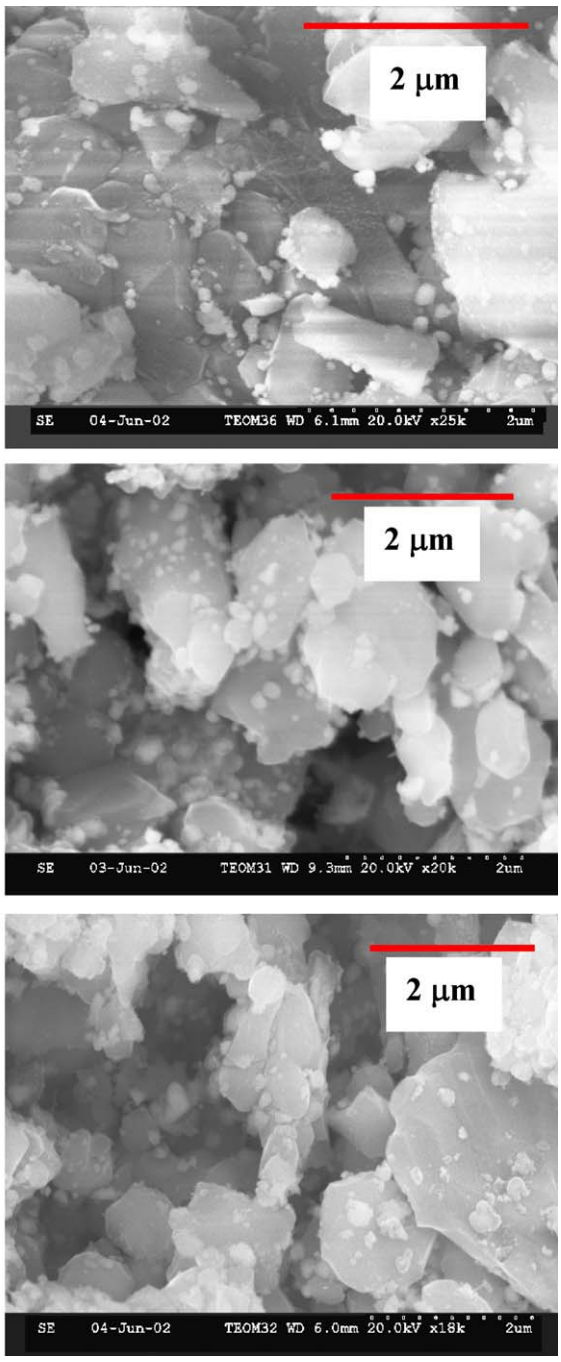

Fig. 8. SEM images of the used ICI catalyst samples after reaction at 1 atm and 650 °C at different feed gas compositions simulating (1) initial CO_2 reforming (CH_4:CO_2:CO:H_2 = 1:1:0:0), 1.5 h. (2) 25% CO_2 reforming conversion (CH_4:CO_2:CO:H_2 = 0.75:0.75:0.5:0.5), 6 min. (3) 50% CO_2 reforming conversion (CH_4:CO_2:CO:H_2 = 0.5:0.5:1:1), 3 min.

carbon has a hollow structure with metal particles on the top of these filaments. The diameter of the filamentous carbon is about 20–50 nm with hollows ranging from 10 nm to 15 nm. The sizes of metal particles on the tip (top) of the filamentous carbon are either similar to the diameter of the filament (Fig. 9(C)) or close to the hollow diameter (Fig. 9(D) and (E)). The shapes of these metal particles are either a sphere (Fig. 9(D) and (E)) or half-sphere with flat bottom (Fig. 9(C)). (F) shows a part of twisted filamentous carbon.

The TEM images of the filaments with Ni metal remaining at the tip (Fig. 9) suggest that the filamentous carbon were formed by carbon diffusion into nickel and lifting nickel out of the catalyst surface, which is consistent with the model described by Baker [35] When more CO contributes to the formation and accumulation of surface carbon species, the metal catalyst surface is encapsulated by a layer of carbon preventing further methane decomposition.

Fig. 10 shows the TEM images of the carbons formed on the Ni/Al_2O_3 (ICI) catalyst sample subjected to 6 min reaction at 1 atm and 650 °C with the feed composition of CH_4:CO_2:CO:H_2 = 0.75:0.75:0.5:0.5. The morphology of carbon shown in Fig. 10(A)–(F) is different from that on the sample discussed above. Besides a few images of filamentous carbon, most of the carbon formed on this sample is encapsulating the spherical metal or support particles (Fig. 10(B)) or encapsulating irregular metal or support particles (Fig. 10(A), (C), and (D)). Although filamentous carbon with hollow structure is again observed on this sample (Fig. 10(E) and (F)), the diameter of this filament is close to 50 nm and the interior diameter of the hollow is very small (<5 nm). Fig. 10(E) shows a complete growing path of a filament from the top to the bottom. The filament seems to grow from a base of encapsulating carbon. Fig. 10(F) shows a filamentous carbon broken due to the supersonic pretreatment during the sample preparation for TEM. The metal particle is actually enclosed inside the filament.

Fig. 11 shows the TEM images of the carbon on the Ni/Al_2O_3 (ICI) catalyst sample after 3 min reaction at 1 atm and 650 °C using the feed of CH_4:CO_2:CO:H_2 = 0.5:0.5:1:1. It is even more difficult to find filamentous carbon on this sample during TEM measurement compared to the above samples. Most of the carbon is found to be encapsulating carbon deposits as shown in Fig. 11(A). However, filamentous carbon or the precursor of filamentous carbon with the diameter of about 30 nm was indeed observed through careful searching during the TEM measurement, as shown in Fig. 11(C). Interestingly, filamentous carbon with the diameter of 130 nm is observed (Fig. 11(B)) as well. The diameter of this filament is similar to the metal particle located at the bottom of the filament. The filament seems to extrude from the bottom metal particles. However, it is not impossible that there is a metal particle covered by carbon layers at the top of the filament which may not be seen clearly by the TEM. The layer structure is discernible with a round shape at the top.

An overall observation from the TEOM measurement is that on the catalyst sample subjected to 6 min reaction at 1 atm and 650 °C at CH_4:CO_2:CO:H_2 = 0.75:0.75:0.5:0.5 and on the catalyst sample subjected to 3 min reaction at 1 atm and 650 °C at CH_4:CO_2:-CO:H_2 = 0.5:0.5:1:1, most of the carbon is found to be encapsulating carbon deposits and there is rarely any filamentous carbon observed. These findings agree well with the TPO-IR experimental results showing that carbon on the catalyst sample after the reaction at CH_4:CO_2:CO:H_2 = 1:1:0:0 has the highest oxidation peak temperature among these three samples.

However, based on all the experimental results discussed above, it is not clear whether more filamentous carbon on the sample treated at CH_4:CO_2:CO:H_2 = 1:1:0:0 is due to the absence of CO in the feed or due to the longer reaction time resulting from the lower carbon formation rate without the presence of CO in the feed. More recent work with detailed TEM characterization of carbon deposits by Zhu et al. [36,37] provided clear supporting evidences that more filamentous carbon is formed from methane decomposition reaction on Ni/Al_2O_3 catalyst [36] and more encapsulating carbon is formed when CO is present during CO_2 reforming of methane on the same Ni/Al_2O_3 catalyst [37].

3.6. Kinetic study of carbon formation on P_{CH_4} and P_{CO} in CO_2 reforming

The TEOM results in Fig. 5 illustrate that CO in the product stream of CO_2 reforming could be another major component

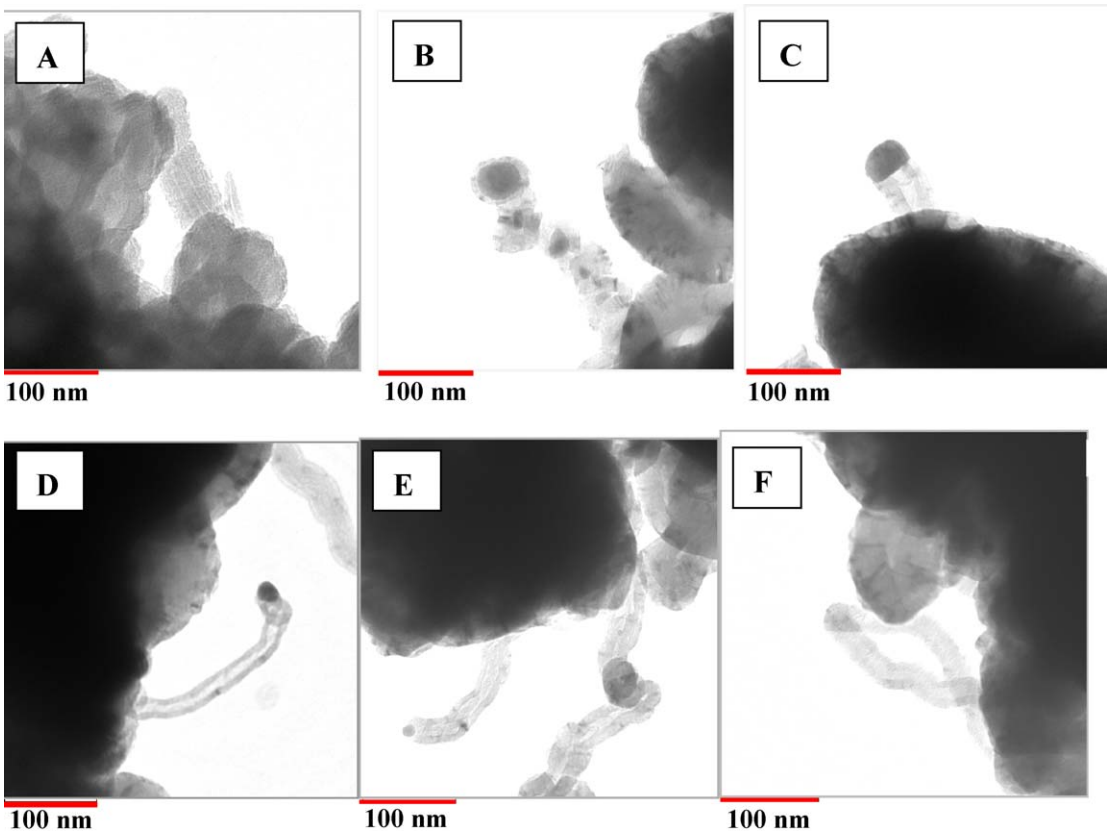

Fig. 9. TEM images of the used Ni/Al_2O_3 (ICI Syntix 23-4) catalyst sample after 1.5 h reaction at 1 atm and 650 °C at feed gas composition simulating initial CO_2 reforming (CH_4:CO_2:CO:H_2 = 1:1:0:0).

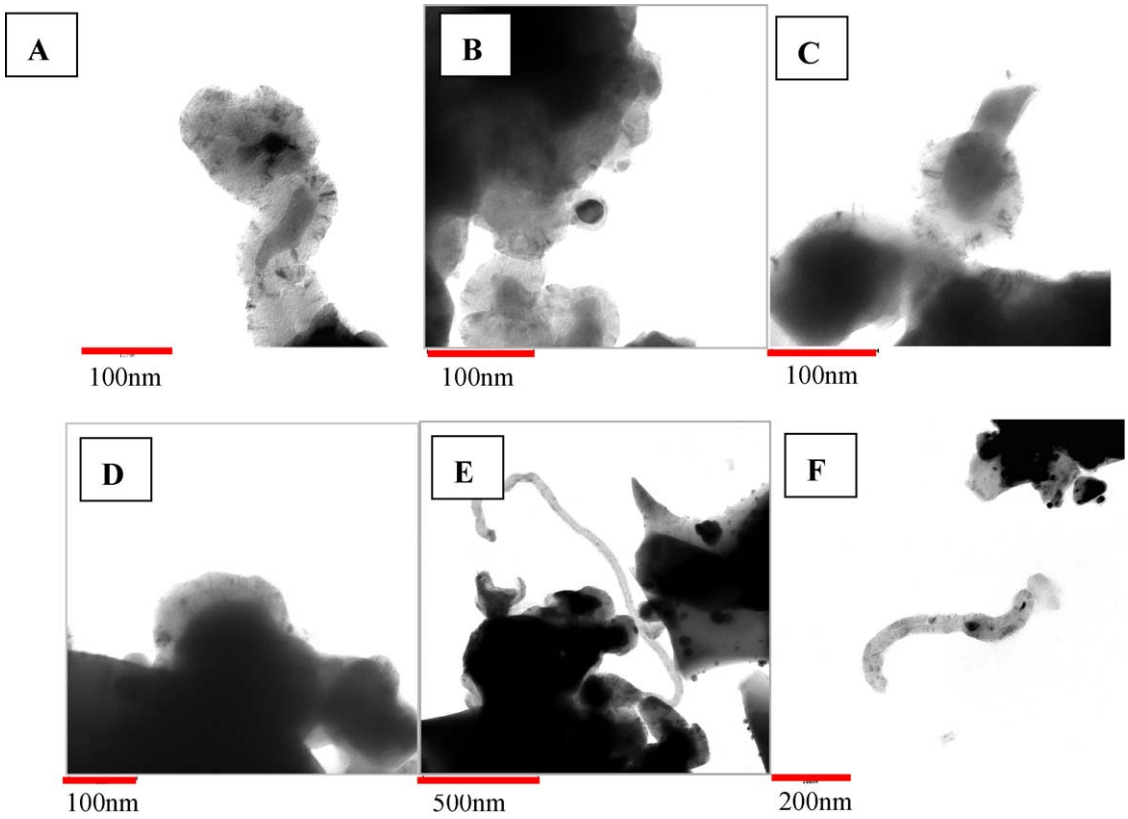

Fig. 10. TEM images of the used Ni/Al_2O_3 (ICI Syntix 23-4) catalyst sample after 6 min reaction at 1 atm and 650 °C at feed gas composition simulating 25% CO_2 reforming conversion (CH_4:CO_2:CO:H_2 = 0.75:0.75:0.5:0.5).

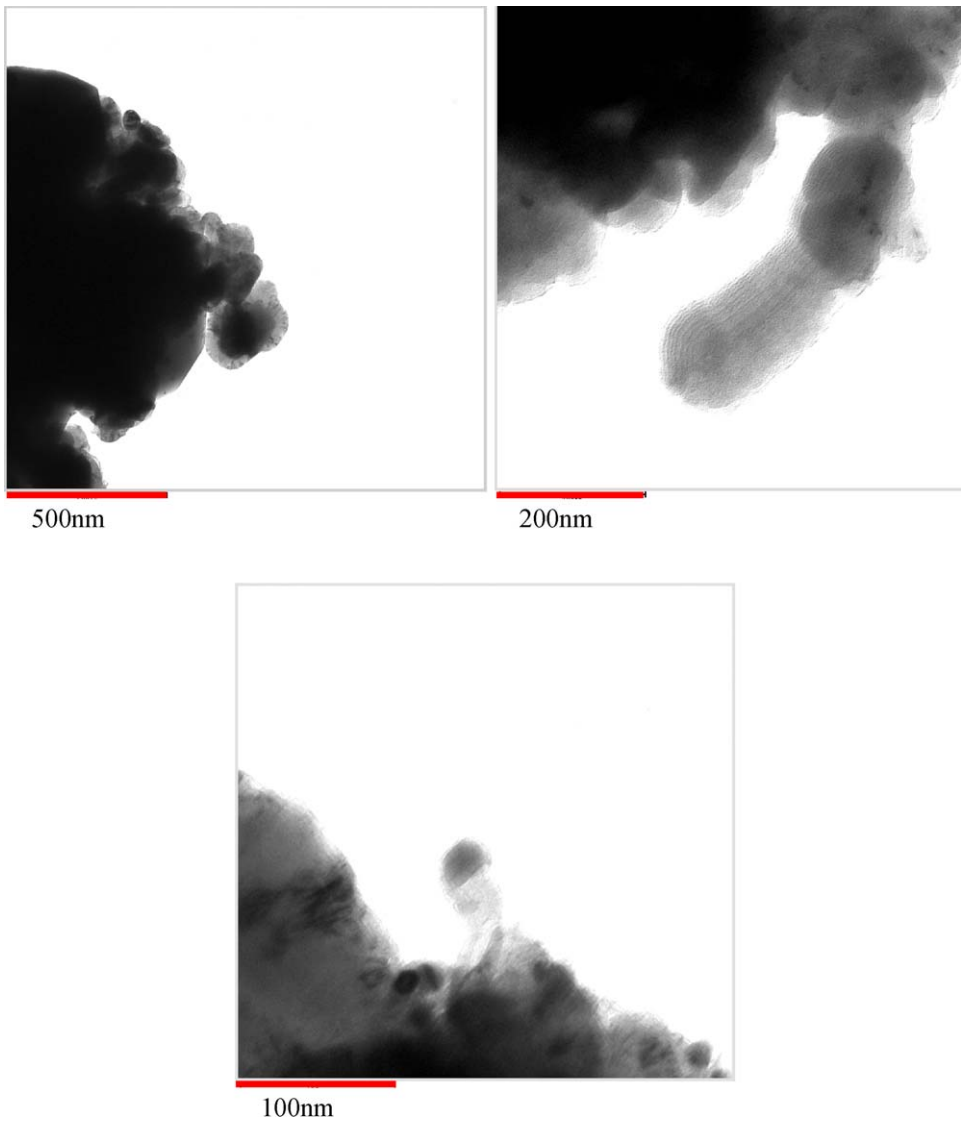

Fig. 11. TEM images of the used Ni/Al_2O_3 (ICI Syntix 23-4) catalyst sample after 3 min reaction at 1 atm and 650 °C at feed gas composition simulating 50% CO_2 reforming conversion (CH_4:CO_2:CO:H_2 = 0.5:0.5:1:1).

contributing to carbon formation during the CO_2 reforming reaction. To further elucidate the contribution of CH_4 and CO to carbon formation, the kinetic study on the effect of partial pressure of CH_4 or CO (P_{CH_4} or P_{CO}) on carbon formation rates was conducted at conditions close to differential conditions at 1 atm and 650 °C.

Fig. 12 shows the rate of carbon formation as a function of P_{CH_4} or P_{CO}. At $P_{CH_4} = 0.062$ atm, $P_{CO_2} = 0.28$ atm, $P_{H_2} = 0.062$ atm, and $P_{(CO+Ar)} = 0.59$ atm, it is found that carbon formation rate only has a very slow increase with the increase of P_{CO} (Fig. 12(1)). No carbon formation was observed until P_{CO} larger than P_{CO_2} (0.28 atm). However, at $P_{CO} = 0.062$ atm, $P_{CO_2} = 0.28$ atm, $P_{H_2} = 0.062$ atm, and $P_{(CH_4+Ar)} = 0.59$ atm, much greater influence of P_{CH_4} on carbon formation rate is evident (Fig. 12(2)) although carbon formation is only observable until P_{CH_4} is above 0.20 atm, which is close to P_{CO_2} (0.28 atm). The difference of the effect of P_{CH_4} and P_{CO} on carbon formation probably results from the inhibition of CO_2 on CO dissociation over Ni catalyst and the promoted CH_4 dissociation on Ni catalysts by the presence of CO_2 or oxygen derived from CO_2 [38]. The surface carbon species from CH_4 dissociation may react with surface oxygen or CO_2 into other gas products such as CO, H_2, and H_2O without the formation of carbon. However, once P_{CH_4} is larger than P_{CO_2}, the extra surface carbon species from CH_4

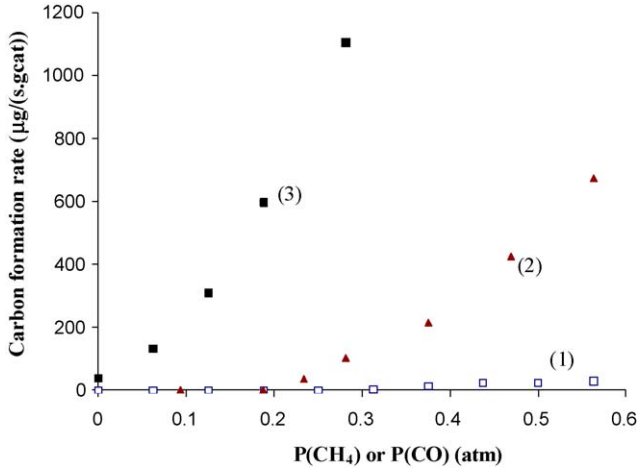

Fig. 12. Carbon formation rates at different P_{CH_4} or P_{CO} at 1 atm and 650 °C over 25 mg Ni/Al_2O_3 (ICI Syntix 23-4) catalyst.
(1) $P_{(CO+Ar)} = 0.59$ atm, $P_{CH_4} = 0.062$ atm, $P_{CO_2} = 0.28$ atm, $P_{H_2} = 0.062$ atm. (2) $P_{(CH_4+Ar)} = 0.59$ atm, $P_{CO} = 0.062$ atm, $P_{CO_2} = 0.28$ atm, $P_{H_2} = 0.062$ atm. (3) $P_{(Ar+CO)} = 0.375$ atm $P_{CH_4} = 0.28$ atm $P_{CO_2} = 0.28$ atm, $P_{H_2} = 0.062$ atm.

dissociation may result in the accumulation of carbon on the catalyst surface and lead to the observed increase of carbon formation rates. Therefore, it is our speculation that the inhibition ability of CO_2 on carbon formation from CO may be weakened if more CH_4 is presented in the system. This speculation is strongly supported by our observation from the following experiment.

When both P_{CH_4} and P_{CO_2} are set to be equal (e.g., both at 0.28 atm), similar to the situation in the equimolar CO_2–CH_4 reforming reaction, it is observed that P_{CO} has the greatest effect on carbon formation rates (Fig. 12(3)). Carbon formation is observed even at P_{CO} = 0.0 atm. Additionally, the effect of P_{CO} on carbon formation rates is more than just the sum of the single effect of P_{CH_4} and P_{CO}. The reaction between CH_4 and CO_2 may weaken the inhibition effect of CO_2 on CO disproportionation and lead to severe carbon formation from CO.

Based on the above results, it is clear that both CH_4 and CO are the sources of carbon formation in CO_2 reforming. CO in the products can become a major source for carbon formation in an equimolar CO_2–CH_4 reforming system. This is consistent with the suggestion by Bradford and Vannice [16].

3.7. Effect of H_2O on carbon formation in CO_2 reforming

By a similar kinetic study, the change of carbon formation rates was investigated by replacing part of CO_2 with H_2O. As shown in Fig. 13, the presence of H_2O can significantly suppress the carbon formation rates from both CH_4 and CO. For example comparing the effect of P_{CO} on carbon formation in the case of $P_{CH_4} = 0.28$ atm and $P_{CO_2} = 0.28$ atm (Fig. 12(3)) and in the case of $P_{CH_4} = 0.28$ atm and $P_{CO_2} = P_{H_2O} = 0.14$ atm (Fig. 13(3)), carbon formation rates increase sharply when P_{CO} increases from 0 atm to 0.3 atm in the former case, while there is barely any carbon formation until P_{CO} = 0.3 atm in the later case.

Therefore, addition of H_2O into the CO_2 reforming system can significantly reduce carbon formation. This is probably due to the stronger ability of H_2O to remove carbon species from both CH_4 and CO. This observation is also consistent with the previously reported advantage of tri-reforming reaction process in eliminating carbon formation [6,7].

3.8. Effect of H_2 and H_2 + CO on carbon formation in CO_2 reforming

We also examined the effects of H_2 and H_2 + CO on carbon formation during CO_2 reforming. Fig. 14 shows the TEOM monitoring of carbon formation with different feeds containing

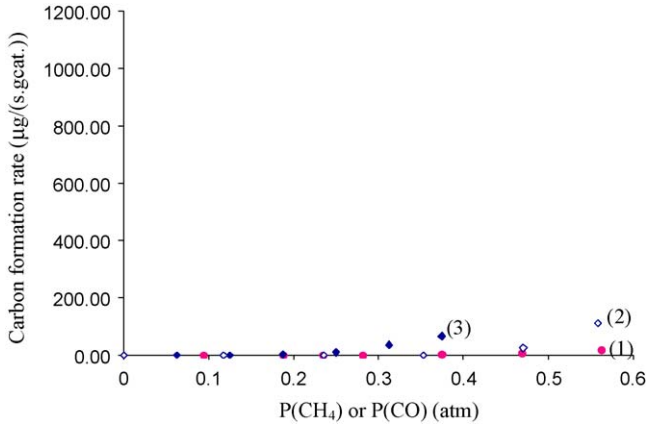

Fig. 13. Carbon formation rates at different P_{CH_4} or P_{CO} at 1 atm and 650 °C over 25 mg Ni/Al_2O_3 (ICI Syntix 23-4) catalyst. (1) $P_{(CH_4+Ar)} = 0.59$ atm, $P_{CO_2} = P_{H_2O} = 0.14$ atm, $P_{H_2} = P_{CO} = 0.062$ atm. (2) $P_{(CO+Ar)} = 0.56$ atm, $P_{CH_4} = 0.12$ atm, $P_{H_2O} = P_{CO_2} = 0.13$ atm, $P_{H_2} = 0.062$ atm. (3) $P_{(CO+Ar)} = 0.38$ atm, $P_{CH_4} = 0.28$ atm, $P_{H_2O} = P_{CO_2} = 0.14$ atm, $P_{H_2} = 0.062$ atm.

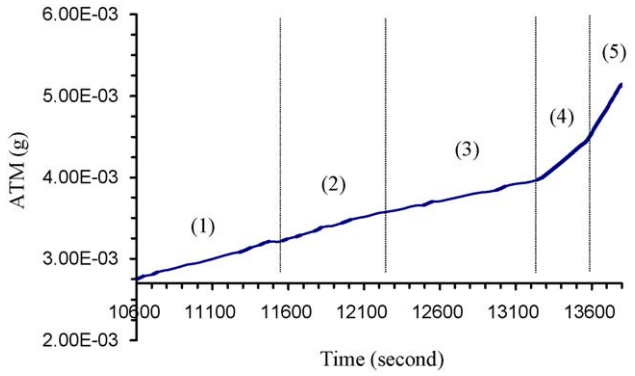

Fig. 14. Carbon formation measurement by TEOM at 650 °C and 1 atm over 25.5 mg Ni/Al_2O_3 (ICI) catalyst after reduction at 650 °C. (1) CH_4:CO_2:H_2:CO:Ar = 1:1:0:0:0.25, CH_4 flow rate = 20 ml/min. (2) CH_4:CO_2:H_2:CO:Ar = 0.9:0.9:0.2:0:0.45, CH_4 flow rate = 18 ml/min. (3) CH_4:CO_2:H_2:CO:Ar = 0.8:0.8:0.4:0:0.65, CH_4 flow rate = 16 ml/min. (4) CH_4:CO_2:H_2:CO:Ar = 0.9:0.9:0.2:0.2:0.25, CH_4 flow rate = 18 ml/min. (5) CH_4:CO_2:H_2:CO:Ar = 0.8:0.8:0.4:0.4:0.25, CH_4 flow rate = 16 ml/min.

H_2 and CO in addition to CH_4 and CO_2 at 650 °C under 1 atm. Compared to the case with CH_4 + CO_2 alone in the feed gas shown in Fig. 14(1), the addition of H_2 in the feed (Fig. 14(2)) and increasing the H_2 partial pressure (Fig. 14(3)) further enhanced the carbon formation. Since H_2 could hydrogenate the surface carbon species to inhibit surface accumulation of carbon, this result seems counter-intuitive. To further clarify this trend, a separate series of TEOM experiments were conducted with CH_4 + H_2 in the feed, and the results are shown in Fig. 15. The TEOM results clearly showed that increasing the H_2 partial pressure enhanced carbon formation from CH_4. The recent work by Zhu et al. [36] clearly showed that filamentous carbon is formed from methane decomposition on Ni/Al_2O_3. Therefore, the present TEOM results showing H_2-enhanced carbon formation from methane suggest that hydrogen gas can help hydrogenate the surface carbon species and clean the surface nickel metal sites active for methane decomposition, thus increasing carbon formation.

On the other hand, the addition of CO in the feed of CO_2 reforming (Fig. 14(4)) and increasing the CO partial pressure (Fig. 14(5)) enhanced the carbon formation to a higher level than that with H_2 addition to CO_2 reforming feed gas. This is consistent with the above results on the importance of CO as a source of carbon formation. We further conducted a separate series of comparative TEOM experiments with pure CO as feed and with CH_4 + CO_2 as the feed, and the results are shown in Fig. 16. The TEOM results clearly showed carbon formation from CO alone is very significant; the amount of carbon formed from CO is almost similar to that with a feed gas containing both CH_4 and CO_2 as is the case for CO_2 reforming of CH_4. This trend again suggests the

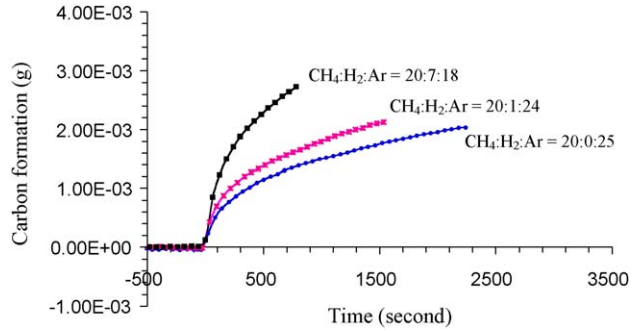

Fig. 15. Carbon formation from methane at different H_2 partial pressures at 650 °C and 1 atm over Ni/Al_2O_3 (ICI) catalyst (26 mg) after reduction at 650 °C.

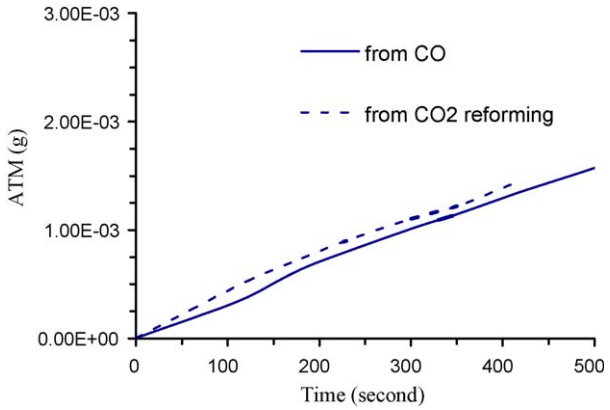

Fig. 16. Carbon formation from CO + Ar and CO_2 reforming at 650 °C and 1 atm over 25.5 mg Ni/Al_2O_3 (ICI) catalyst after reduction at 650 °C. In both cases, CO concentrations are the same. Case 1: CO + Ar (CO flow rate = 10 ml/min, Ar flow rate = 40 ml/min). Case 2: CO_2 reforming (CH_4:CO_2:H_2:CO = 15:15:10:10, CH_4 flow rate = 15 ml/min).

importance of CO as a major source of carbon formation during CO_2 reforming.

4. Conclusion

TEOM results and kinetic study on carbon formation have established that both CH_4 in the reactants and CO in the products can be the source of carbon formation in the CO_2 reforming reaction. In an equimolar CO_2–CH_4 reforming condition, CO in the product stream is likely the major source of carbon formation. High-resolution TEM and TPO-IR revealed that carbon formed in CO_2 reforming from a feed without containing CO shows more filamentous carbon, which is more difficult to be oxidized, while carbon formed from a feed containing CO mostly encapsulates metal particles in the catalyst and is relatively easy to be oxidized.

TEOM results also revealed that H_2 addition to the feed gas containing either CH_4 or $CH_4 + CO_2$ can enhance carbon formation from methane, probably by hydrogenating surface carbon species and clean the surface metal sites active for methane decomposition. Addition of $H_2 + CO$ to the feed gas $CH_4 + CO_2$ can further enhance carbon formation more than that with H_2 addition alone.

Replacing some of CO_2 with H_2O may greatly inhibit carbon formation encountered in CO_2 reforming. Kinetic study with TEOM shows that H_2O can reduce carbon formation from both CO and CH_4.

The present TEOM results further rationalize the demonstrated advantage for eliminating carbon formation in the tri-reforming process recently proposed from our laboratory [6,7] and established by many independent studies [8–11], where a synergetic combination of CO_2 reforming, steam reforming and partial oxidation of methane can produce industrially useful syngas with desired H_2/CO ratios without carbon formation problem [4].

Acknowledgments

The authors wish to acknowledge the US Department of Energy National Energy Technology Laboratory for partial financial support of this work. The authors would also like to thank Dr. M.A. Vannice and Dr. S. Eser of PSU for the helpful discussions.

References

[1] M. Aresta (Ed.), Carbon Dioxide Recovery and Utilization, Springer, New York, 2003.
[2] CO_2 Conversion and Utilization, American Chemical Society Publication, ACS Symposium Series, Washington, DC, 2003.
[3] C.-J. Liu, R.G. Mallinson, M. Aresta (Eds.), Utilization of Greenhouse Gases, American Chemical Society Publication, ACS Symposium Series, Washington, DC, 2003
[4] C.S. Song, Catal. Today 115 (2006) 2–32.
[5] A.T. Ashcroft, A.K. Cheetham, M.L.H. Green, P.D.F. Vernon, Nature 352 (1991) 225–226.
[6] C.S. Song, W. Pan, Catal. Today 98 (2004) 463–484.
[7] C.S. Song, Chem. Innov. 31 (2001) 21–26.
[8] M. Halmann, A. Steinfeld, Catal. Today 115 (2006) 170–178.
[9] H. Jiang, H. Li, H. Xu, Y. Zhang, Fuel Proc. Technol. 88 (2007) 988–995.
[10] J.S. Kang, D.H. Kim, S.D. Lee, S.I. Hong, D.J. Moon, Appl. Catal. A: Gen. 332 (2007) 153–158.
[11] W.J. Cho, T.Y. Song, A. Mitsos, J.T. McKinnon, G.H. Ko, J.E. Tolsma, D. Denholm, T. Park, Catal. Today 139 (2009) 261–267.
[12] M.C.J. Bradford, M.A. Vannice, Catal. Rev. 41 (1999) 1–42.
[13] Y.H. Hu, E. Ruckenstein, Adv. Catal. 48 (2004) 297.
[14] S. Wang, G.Q. Lu, Energy Fuels 12 (1998) 1235–1240.
[15] K. Tomishige, Y.G. Chen, K. Fujimoto, J. Catal. 181 (1999) 91–103.
[16] M.C.J. Bradford, M.A. Vannice, Appl. Catal. A 142 (1996) 73–96.
[17] J.T. Richardson, S.A. Paripatyadar, Appl. Catal. 61 (1990) 293–309.
[18] Z.L. Zhang, X.E. Verykios, Catal. Today 21 (1994) 589–595.
[19] R.T.K. Baker, P.S. Harris, in: P.L. Walker, P.A. Thrower (Eds.), The Formation of Filamentous Carbon in Chemistry and Physics of Carbon, vol. 14, 1978, pp. 83–165.
[20] K. Tomishige, Y. Himeno, Y. Matsuo, Y. Yoshinaga, K. Fujimoto, Ind. Eng. Chem. Res. 39 (2000) 1891–1897.
[21] H.M. Swaan, V.C.H. Kroll, G.A. Martin, C. Mirodatos, Catal. Today 21 (1994) 571–578.
[22] U. Olsbye, T. Wurzel, L. Mleczko, Ind. Eng. Chem. Res. 36 (1997) 5180–5188.
[23] P.E. Nolan, D.C. Lynch, A.H. Cutler, J. Phys. Chem. B 102 (1998) 4165–4175.
[24] M.C. Demicheli, E.N. Ponzi, O.A. Ferretti, A.A. Yeramian, Chem. Eng. J. Biochem. Eng. 46 (1991) 129–136.
[25] V.C.H. Kroll, H.M. Swaan, C. Mirodatos, J. Catal. 161 (1996) 409–422.
[26] F.J. Dent, L.A. Moignard, A.H. Eastwood, W.H. Blackburn, D. Heeden, An investigation into the catalytic synthesis of methane, 1945–1946 London, pp. 604–693.
[27] J.R. Rostrup-Nielsen, J. Catal. 27 (1972) 343–356.
[28] K. Denbigh, The Principles of Chemical Equilibrium, 3rd ed., Cambridge University Press, Cambridge, Great Britain, 1971, p. 494.
[29] G.W. Bridger, G.C. Chinchen, Hydrocarbon-reforming Catalysts (Chapter 5), Catalyst Handbook—with Special Reference to Unit Processes in Ammonia and Hydrogen Manufacture, Springer-Verlag, New York, 1970, pp. 63–96.
[30] J.S. Chang, S.E. Park, H. Chon, Appl. Catal. A: Gen. 145 (1996) 111–124.
[31] M.A. Goula, A.A. Lemonidou, A.M. Efstathiou, J. Catal. 161 (1996) 626–640.
[32] U. Olsbye, O. Moen, A. Slagtern, I.M. Dahl, Appl. Catal. A: Gen. 228 (2002) 289–303.
[33] A. Shamsi, C.D. Johnson, Am. Chem. Soc. Div. Fuel Chem. Prepr. 221 (2001) 49.
[34] S. Wang, G.Q.M. Lu, Appl. Catal. B: Environ. 16 (1998) 269–277.
[35] R.T.K. Baker, Carbon 27 (1989) 315–323.
[36] X.L. Zhu, D.G. Cheng, P.Y. Kuai, Energy Fuels 22 (2008) 1480–1484.
[37] X.L. Zhu, P.P. Huo, Y.P. Zhang, D.G. Cheng, C.J. Liu, Appl. Catal. B 81 (2008) 132–140.
[38] J.Z. Luo, L.Z. Gao, C.F. Ng, C.T. Au, Catal. Lett. 62 (1999) 153–158.